

See discussions, stats, and author profiles for this publication at: <https://www.researchgate.net/publication/263942488>

# Tailored Parallel Graphene Stripes in Plastic Film with Conductive Anisotropy by Shear-Induced Self-Assembly

ARTICLE *in* JOURNAL OF PHYSICAL CHEMISTRY LETTERS · DECEMBER 2012

Impact Factor: 7.46 · DOI: 10.1021/jz301811b

---

CITATIONS

9

---

READS

50

6 AUTHORS, INCLUDING:



Yutian Zhu

Chinese Academy of Sciences

43 PUBLICATIONS 356 CITATIONS

SEE PROFILE

# Tailored Parallel Graphene Stripes in Plastic Film with Conductive Anisotropy by Shear-Induced Self-Assembly

Cui Mao,<sup>†,‡</sup> Jinrui Huang,<sup>†,‡</sup> Yutian Zhu,<sup>\*,†</sup> Wei Jiang,<sup>\*,†</sup> Qingxin Tang,<sup>§</sup> and Xiaojing Ma<sup>†</sup>

<sup>†</sup>State Key Laboratory of Polymer Physics and Chemistry, Changchun Institute of Applied Chemistry, Chinese Academy of Sciences, Changchun 130022, P. R. China

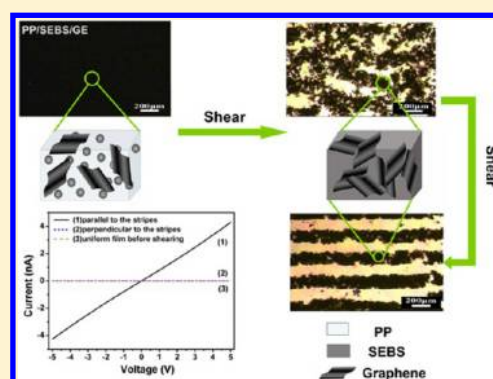
<sup>‡</sup>Graduate School of Chinese Academy of Sciences, Beijing 100049, P. R. China

<sup>§</sup>Key Laboratory of UV Light Emitting Materials and Technology under Ministry of Education, Northeast Normal University, Changchun 130024, P. R. China

## Supporting Information

**ABSTRACT:** We present a simple but efficient route to prepare a highly anisotropic conductive plastic thin film from the polypropylene/(styrene-ethylene/butadiene-styrene) triblock copolymer/graphene blend via shear-induced self-assembly. Under the shear-flow induction, GE nanosheets dispersed in the polymer matrix can spontaneously assemble into ordered parallel stripes, which endow the materials significantly conductive anisotropy. The electrical resistivity in the direction parallel to the graphene stripes is almost four orders of magnitude lower than that which is perpendicular to the stripes. This study provides a new method for the precise control of the organization of functional nano-objects in polymer matrix, which can be widely extended to the fabrication of other multifunctional anisotropic materials of interest in various fields.

**SECTION:** Physical Processes in Nanomaterials and Nanostructures



The fabrication of ordered microscale structures from the self-assembly of functional objects on the nanometer scale has attracted considerable attention because of their fundamental and technological significance.<sup>1</sup> The performance of the nanomaterials can be considerably enhanced when the functional nano-objects build larger hierarchical architectures with unique morphologies, orientations, and dimensions.<sup>2–4</sup> The properties of such materials can be fine-tuned by changing their structure and morphology. Therefore, much effort has been made to precisely control the organization of functional nano-objects, especially in the formation of ordered 1D chain- or stripe-like assemblies because of their desirable anisotropic properties in electronic and optical devices.<sup>5–7</sup> Several techniques including magnetic-field-induced assembly,<sup>1,8,9</sup> electric-field-induced assembly,<sup>10–12</sup> self-assembly of block copolymers with nanoparticles,<sup>13–17</sup> and templated synthesis<sup>18</sup> have been exploited to produce these 1D structured materials. However, a facile and universal method for constructing such nanostructures from various functional nano-objects in a polymer matrix remains a challenge. Driven by the requirements of multifunctional polymer nanocomposites, simple and straightforward methods are urgently needed to precisely organize nanofillers into a well-ordered 1D structure in the polymer matrix. Shear flow, which was found to induce the formation of the ordered morphologies,<sup>19–24</sup> is an promising new method for such anisotropic chain- or stripe-like structures in the polymer matrix. Although a great number of

investigations have been carried out on the formation of shear-induced patterns, this technique was rarely used in the material sciences because these shear-induced patterns were in a metastable state. Once the shear field is changed or removed, so does the shear-induced patterns. Our previous work<sup>25</sup> demonstrated that the dispersed polyamide 6 (PA6) and the styrene-ethylene/butadiene-styrene triblock copolymer (SEBS) can spontaneously self-organize into a relatively stable and well-ordered parallel-cluster structure in a polypropylene (PP) matrix under simple shear flow. If the conductive nanofillers are used to replace the dispersed PA6, then they may also form this shear-induced parallel-cluster structure in the polymer matrix, which can be then frozen to fabricate the highly anisotropic conductive plastic materials.

Graphene is a very promising new material in nanoscience because of its extraordinary mechanical,<sup>26</sup> thermal,<sup>27</sup> and electrical properties.<sup>28</sup> Graphene has various potential applications in conductive composites,<sup>29,30</sup> energy devices,<sup>31,32</sup> sensors,<sup>33</sup> electronics,<sup>34</sup> and so on since its discovery in 2004. In this letter, we present the simple technique of shear-flow-induced self-assembly to fabricate plastic films that contain well-ordered parallel graphene stripes in a PP/SEBS/graphene blend. Under the induction of shear flow, graphene nanosheets

**Received:** November 7, 2012

**Accepted:** December 11, 2012

**Scheme 1. Illustration of the Evolutionary Process during the Formation of the Parallel GE Stripes from the PP/SEBS/GE Blend under Shear Flow**

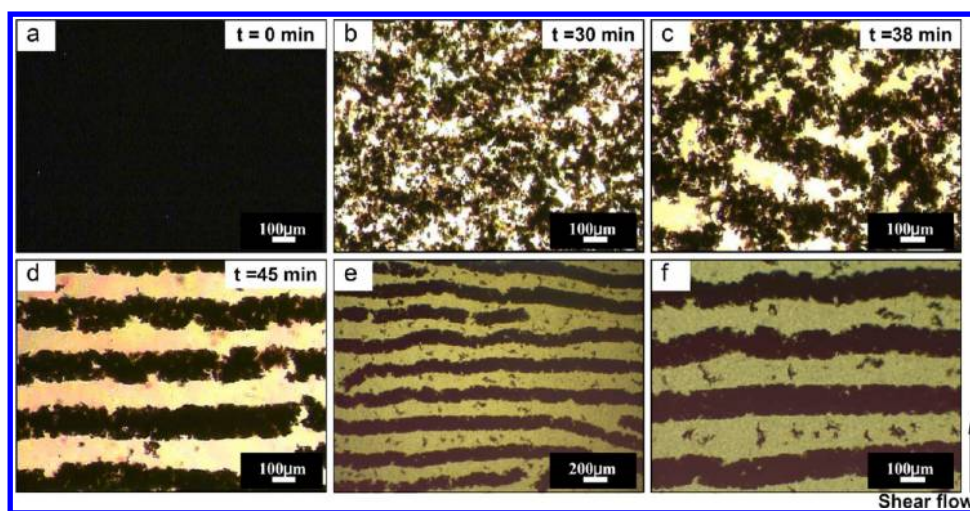
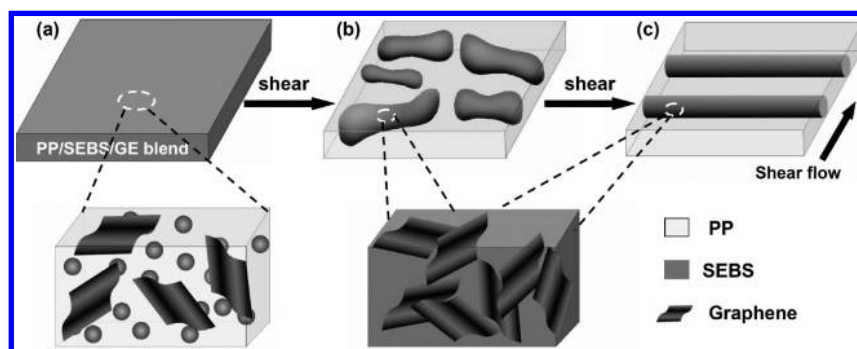


**Figure 1.** Optical micrographs of the morphological evolution of the PP/SEBS/GE composite under the shear flow: (a) PP/SEBS/GE composite at 280 °C before shear-induced assembly; (b–d) parallel stripes formation at 280 °C at a shear rate of 0.15 s<sup>−1</sup> and a gap of 250 μm; and (e,f) thin film obtained after cessation of the flow and cooling to the room temperature. The weight ratio of PP/SEBS is 9:1, and the content of GE is 1.5 wt %.

can spontaneously aggregate into aligned parallel stripes that are perpendicular to the flow direction. After the cessation of flow, the parallel graphene stripes can be frozen by decreasing the temperature to below the glass-transition temperature of PP. Such plastic films with the ordered parallel graphene stripes display significant anisotropy in conductivity because of the superior electrical properties of graphene. The electrical resistivity in the direction vertical to the graphene stripes is almost four orders of magnitude higher than that in the horizontal direction. This novel technique, designated as the shear-flow-induced self-assembly, offers a simple but effective route for the formation of larger ordered architectures from various functional nano-objects.

In this letter, graphene (GE) was functionalized by octadecylamine to improve its compatibility with the polymer matrix. Two steps are involved to fabricate the anisotropic thin film with parallel GE stripes, as illustrated in Scheme 1. In the first step, the PP/SEBS/GE composites were prepared by solution-blending, which was followed by compression molding into plate-shapes. Both GE and SEBS were uniformly distributed in the PP matrix, as illustrated in Scheme 1a. In the second step, the hot-pressed plate of the PP/SEBS/GE composite was placed on a Linkam CSS450 shear stage and heated to 280 °C. An Olympus BX-51 optical microscope that was coupled to a digital video camera was used to observe the evolution of the morphology during the shearing process. After

shearing at the proper gap and shear rate, the GE nanosheets started to organize themselves, first into microscale assemblies (Scheme 1b) and finally into the parallel stripes (Scheme 1c) that were perpendicular to the direction of the shear flow. Subsequently, the plastic thin film with the well-ordered parallel GE stripes was obtained after the flow ceased and the film temperature was lowered to room temperature.

In Figure 1, we present a series of optical micrographs to elucidate the formation and evolution of the well-ordered parallel GE stripes under shear flow. During the shearing process, the gap between the two disks of the shear stage is fixed at 250 μm, and the shear rate is fixed at 0.15 s<sup>−1</sup>. The temperature remains constant at 280 °C. Figure 1a shows the initial state of the PP/SEBS/GE composites. Under the microscope, this sample is black and opaque to light, which implies that the GE nanosheets are uniformly distributed in the polymer matrix. Graphene is functionalized by octadecylamine, such that the long nonpolar octadecyl chains graft onto the GE surface. This hydrophobic property causes GE to disperse uniformly in the polymer matrix without agglomeration. After 30 min of shearing, GE and SEBS start to aggregate into short assemblies that are randomly distributed in PP matrix, as shown in Figure 1b. By further increasing the shear time, the short assemblies aggregate into larger assemblies (Figure 1c) until they finally form the well-ordered parallel GE stripes that are aligned perpendicular to the shear flow (Figure 1d). For a full



understanding of the formation mechanism of the GE stripes, we give a video showing the dynamic process of the growth of the GE stripes (Movie S1, Supporting Information). After stopping the shear flow and cooling the sample to room temperature, we have successfully fabricated the plastic thin film with significant anisotropy. Figure 1e,f presents the optical micrographs of the resulting thin film at room temperature under different magnifications. The ordered parallel GE stripes remain unchanged after the cessation of shear flow and the subsequent cooling process. These GE stripes are composed of GE and SEBS aggregates, which are  $\sim 150\ \mu\text{m}$  wide and have an average length of 2.36 mm. The length distribution of the shear-induced GE stripes is given in the Supporting Information (Figure S1). In addition, the regions outside the GE stripes are very transparent, thereby indicating that almost all of the GE nanosheets have assembled into the stripes.

The driving force for the formation of the structures perpendicular to the shear direction, which is the vorticity direction, was previously investigated by Montesi et al.<sup>35</sup> and in our previous work.<sup>25</sup> The formation of clusters or stripes perpendicular to the flow direction is attributed to the existence of negative normal stresses ( $NI$ ). The dispersed phase, which is an aggregate of GE and SEBS, is subjected to the compression effect in the flow direction by the shear flow when  $NI < 0$ . This aggregate is also compressed in the gradient direction because of the confinement effect that is imposed by the upper and lower disks in the shear stage. Consequently, the aggregate can only grow and align along the vorticity direction, which is the direction perpendicular to the shear flow. According to this mechanism, two important factors determine the formation of parallel GE stripes along the vorticity direction. First, SEBS influences the formation of the ordered GE stripes. Small SEBS domains tend to coalesce into bigger domains under a shearing rate of  $0.15\ \text{s}^{-1}$ . During the coalescence, GE nanosheets likewise integrate into the SEBS phase and form the aggregates of SEBS and GE. Therefore, SEBS functions as an “adhesive” in the buildup of GE stripes. Second, the applied shear rate is a key factor for the formation of GE stripes. The optimal shear rate for the well-ordered parallel stripes is in the range of about  $0.1$  to  $0.2\ \text{s}^{-1}$  when the gap is fixed at  $250\ \mu\text{m}$ . This phenomenon may be ascribed to the  $NI$ , which is negative only within this range of shear rate.

Scanning electron microscopy (SEM) and transmission electron microscopy (TEM) were utilized to visualize the internal structure of the GE stripes in the PP/SEBS/GE film. In Figure 2a,b, we present the SEM images of the fractured surfaces of the GE stripes in the obtained plastic thin film. From the fractured surface images, these stripes are found to be cylinders embedded in the PP thin film. The diameters of the stripes are roughly equal to the film thickness. Moreover, these cylinders that are composed of the SEBS and GE nanosheets are comparatively loose as compared with the PP matrix. The dispersion and distribution of GE nanosheets inside the GE/SEBS cylinders were further examined by TEM technique. From the TEM images (Figure 2c,d), it is clear that the GE nanosheets are enriched and randomly distributed in the SEBS phase after the shear induction. Considering the high conductivity of GE, we predict that the resulting thin film with the well-ordered parallel GE stripes will display significant anisotropy in conductivity. To confirm this prediction, we obtained the respective electrical resistivities of the film in the directions parallel and perpendicular to the stripes from the current versus voltage ( $I$ – $V$ ) measurements. The results are

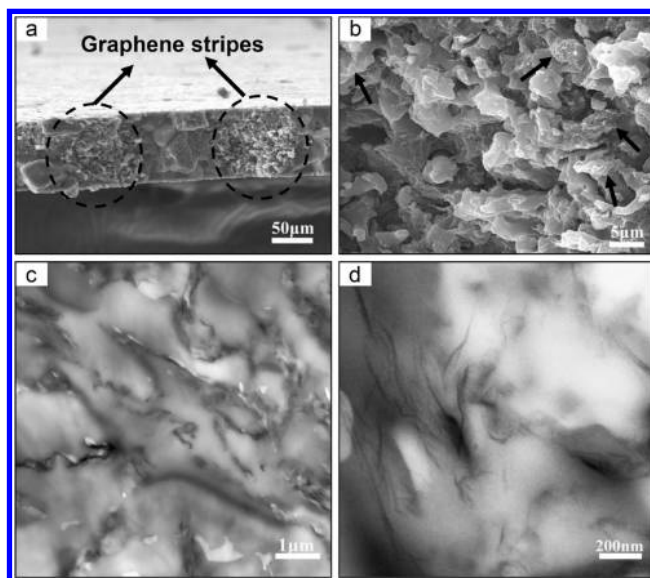


**Figure 2.** SEM and TEM images of the assembled GE stripes composed of GE and SEBS in the anisotropic thin film that was obtained after the shear-induced assembly. SEM images (a,b) are taken from the fractured surface perpendicular to the film plane. (b) Partially enlarged images of panel a. The black arrows in panel b point to GE nanosheets. TEM images (c,d) are the cross-section view by microtome sectioning perpendicular to the GE stripes.

presented in Figure 3. Figure 3a shows a schematic of the  $I$ – $V$  measurement, wherein the Au electrodes are patterned on top of the film. From Figure 3b, the  $I$ – $V$  curve that was measured in the direction parallel to the GE stripes (curve 1 in Figure 3b) exhibits linear Ohmic behavior, thereby indicating that the conductive pathway is formed in this direction because of the GE aggregation inside the stripes. In the direction perpendicular to the stripes (curve 2 in Figure 3b), however, insulating behavior is observed from the measured curve. According to the  $I$ – $V$  curves, the determined electrical resistivity parallel to the GE stripes is  $\sim 3.5 \times 10^5\ \Omega\ \text{m}$ , which is in the range of semiconductors. However, the electrical resistivity perpendicular to the stripes is  $\sim 5.0 \times 10^9\ \Omega\ \text{m}$ , which is almost four orders of magnitude higher than that of the values parallel to the stripes. We also measure the  $I$ – $V$  curve of the PP/SEBS/GE film before the shearing-induced assembly (curve 3 in Figure 3b). On the basis of the corresponding optical image shown in Figure 2a, the GE nanosheets are known to be uniformly distributed in the polymer matrix before shearing and the film is isotropic. Similarly, the composite exhibits insulating behavior with an electrical resistivity of  $\sim 7.4 \times 10^9\ \Omega\ \text{m}$ . This result implies that the GE content (1.5 wt %) is lower than its percolation threshold in PP.

In conclusion, we have demonstrated the self-assembly of GE nanosheets into well-ordered parallel stripes that are perpendicular to the shear direction in a polymer matrix under the shear field. The self-assembly is a spontaneous process driven by the external shear field. The alignment of GE stripes causes the obtained plastic thin film to display highly conductive anisotropy; that is, the electrical resistivity in the direction parallel to the GE stripes is almost four orders of magnitude lower than that which is perpendicular to the stripes. This result indicates that whereas the shear-induced structures are in a metastable state the shear field still can be a promising tool to the design of multifunctional anisotropic materials,

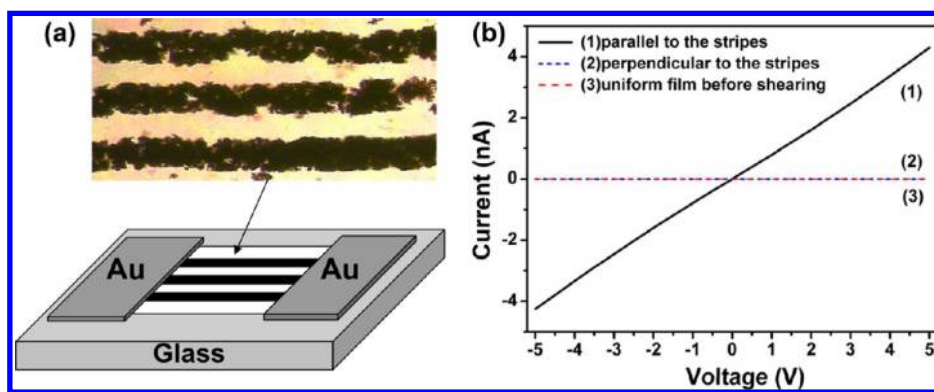


**Figure 3.** (a) Schematic picture of the current versus voltage ( $I$ – $V$ ) measurement with the Au electrodes patterned on top of the film. (b)  $I$ – $V$  curves of the PP/SEBS/GE film obtained after shearing in the directions (1) parallel and (2) perpendicular to the stripes. (3)  $I$ – $V$  curve of the uniform PP/SEBS/GE film before shear-induced assembly.

which offers an alternative to most of the commonly used magnetic-field-induced assembly, especially for the assembly of nonmagnetic nano-objects. Moreover, this approach should work on most nano-objects to the fabrication of multifunctional anisotropic plastic materials of interest in various fields.

## EXPERIMENTAL METHODS

**Materials.** PP (140) was supplied by Jilin Petrochemical (China). The average molecular weight ( $M_n$ ) is  $7.74 \times 10^4$  g mol $^{-1}$ , and the polydispersity index ( $M_w/M_n$ ) is 5.47, respectively. Styrene-ethylene/butadiene-styrene triblock copolymer (SEBS, Kraton G1652;  $M_w$ : ca. 45 000 g mol $^{-1}$ ; styrene content: ca. 29 wt %) was obtained from the Shell Development. In the current study, GE was obtained by modifying graphene oxide with octadecylamine and then reducing it with hydroquinone. The detailed information for the synthesis and characterization of GE was previously reported.<sup>36</sup>

**Preparation of PP/SEBS/GE Composites.** PP/SEBS/GE composites were prepared by solution blending. The weight ratio of PP to SEBS was 9:1, and the loading content of GE was fixed at 1.5 wt % in the composites. First, the desired amount of PP and SEBS was dissolved in toluene at 130 °C under constant stirring. The predetermined amount of GE was dispersed in toluene (0.5 mg mL $^{-1}$ ) and exfoliated by bath sonication (KQ3200DE, 150 W) at room temperature for 1 h. The suspension of GE was then combined with the PP/SEBS solution and heated to 130 °C for 3 h with mechanical stirring. Finally, the solution was slowly added to a large volume of acetone to coagulate the composites with vigorous stirring. The precipitate was filtered and dried in vacuum at 80 °C for 24 h. The dried product was hot-pressed into 0.8 mm thick plates that were 25 mm in diameter at ca. 200 °C and ca. 10 MPa for 10 min.

**Fabrication of PP/SEBS/GE Anisotropic Conductive Film.** The PP/SEBS/GE anisotropic conductive film was prepared by employing a Linkam CSS 450 stage equipped with an Olympus BX-51 optical microscope. The microscopic structures during the shear process were visualized in this manner. The sample was held in the gap between the two quartz disks and was sheared by rotating the bottom disk using a precise motor while the top disk remained stationary. The internal surfaces of the quartz disks were covered with the thin polyimide films to prevent adhesion of the PP/SEBS/GE composites to the quartz disks. The experiments were performed at  $(280 \pm 1)$  °C. The

gap was fixed at 250  $\mu$ m, and the applied shear rate was kept constant at 0.15 s $^{-1}$ . After shearing for  $\sim$ 45 min, GE that was distributed in the matrix was aggregated into the ordered parallel stripes. Thereafter, this ordered structure was maintained by decreasing the stage temperature. The resulting anisotropic thin film was peeled from the polyimide film at room temperature.

**Thin Film Characterization.** To explore the structure and morphology of the thin film, we examined the sample by SEM using an XL30 ESEM (FEG, Micro FEI PHILIPS) at an acceleration voltage of 100 kV. The thin film was first fractured in liquid nitrogen and then sputter-coated with a thin layer of gold to prepare the samples for SEM. The presented image was obtained from the fractured surface that was perpendicular to the film plane. TEM was also used to characterize the internal structure of GE stripes. The GE stripes were embedded in epoxy resin (Epon); then, the thin sections of about 50 nm thickness of the resin sample were obtained at a temperature of  $-80$  °C using a microtome (LEICA ULTRACUTR ME1-057) equipped with a glass knife. TEM measurements were performed on a JEOL JEM-1011 transmission electron microscope operated at an acceleration voltage of 100 kV.

To characterize the current versus voltage ( $I$ – $V$ ) curves, we sputtered gold electrodes (2.0 mm  $\times$  0.5 mm) onto the film with a spacing of 1.5 mm in the directions parallel and perpendicular to the GE stripes. Two-point-probe measurements were performed to obtain the  $I$ – $V$  curves using a computer-controlled Keithley 4200 semiconductor parameter analyzer at room temperature. The same procedures were performed for the  $I$ – $V$  measurements of the film before the shear-induced self-assembly.

## ASSOCIATED CONTENT

### Supporting Information

Histogram of the length distribution of GE stripes and a movie showing the dynamic process of the formation of GE stripes. This material is available free of charge via the Internet at <http://pubs.acs.org>.

## AUTHOR INFORMATION

### Corresponding Author

\*E-mail: ytzhu@ciac.jl.cn (Y.Z.); wjiang@ciac.jl.cn (W.J.). Tel: +86-43185262866. Fax: +86-43185262126.

### Notes

The authors declare no competing financial interest.

## ACKNOWLEDGMENTS

This work was financially supported by the National Natural Science Foundation of China for Youth Science Funds (21104083), Major Program (50930001) and the Scientific Development Program of Jilin Province (201201007).

## REFERENCES

- (1) Amali, A. J.; Saravanan, P.; Rana, R. K. Tailored Anisotropic Magnetic Chain Structures Hierarchically Assembled from Magneto-responsive and Fluorescent Components. *Angew. Chem., Int. Ed.* **2011**, *50*, 1318–1321.
- (2) Ansari, S.; Kellarakis, A.; Estevez, L.; Giannelis, E. P. Oriented Arrays of Graphene in a Polymer Matrix by in situ Reduction of Graphite Oxide Nanosheets. *Small* **2010**, *6*, 205–209.
- (3) Sun, S. H. Recent Advances in Chemical Synthesis, Self-Assembly, and Applications of FePt Nanoparticles. *Adv. Mater.* **2006**, *18*, 393–403.
- (4) Erb, R. M.; Son, H. S.; Samanta, B.; Rotello, V. M.; Yellen, B. B. Magnetic Assembly of Colloidal Superstructures with Multipole Symmetry. *Nature* **2009**, *457*, 999–1002.
- (5) Braun, E.; Eichen, Y.; Sivan, U.; Ben-Yoseph, G. DNA-Templated Assembly and Electrode Attachment of a Conducting Silver Wire. *Nature* **1998**, *391*, 775–778.
- (6) Tang, Z. Y.; Kotov, N. A. One-Dimensional Assemblies of Nanoparticles: Preparation, Properties, and Promise. *Adv. Mater.* **2005**, *17*, 951–962.
- (7) Gong, J. Y.; Li, S. Z.; Zhang, D.; Zhang, X. B.; Liu, C.; Tong, Z. W. High Quality Self-Assembly Magnetite (Fe<sub>3</sub>O<sub>4</sub>) Chain-like Core-Shell Nanowires with Luminescence Synthesized by a Facile One-Pot Hydrothermal Process. *Chem. Commun.* **2010**, *46*, 3514–3516.
- (8) Shen, J. H.; Zhu, Y. H.; Zhou, K. F.; Yang, X. L.; Li, C. Z. Tailored Anisotropic Magnetic Conductive Film Assembled from Graphene-Encapsulated Multifunctional Magnetic Composite Microspheres. *J. Mater. Chem.* **2012**, *22*, 545–550.
- (9) Fragouli, D.; Buonsanti, R.; Bertoni, G.; Sangregorio, C.; Innocenti, C.; Falqui, A.; Gatteschi, D.; Cozzoli, P. D.; Athanassiou, A.; Cingolani, R. Dynamical Formation of Spatially Localized Arrays of Aligned Nanowires in Plastic Films with Magnetic Anisotropy. *ACS Nano* **2010**, *4*, 1873–1878.
- (10) Cardinali, M.; Valentini, L.; Kenny, J. M. Anisotropic Electrical Transport Properties of Graphene Nanoplatelets/Pyrene Composites by Electric-Field-Assisted Thermal Annealing. *J. Phys. Chem. C* **2011**, *115*, 16652–16656.
- (11) Martin, C. A.; Sandler, J. K. W.; Windle, A. H.; Schwarz, M. K.; Bauhofer, W.; Schulte, K.; Shaffer, M. S. P. Electric Field-Induced Aligned Multi-Wall Carbon Nanotube Networks in Epoxy Composites. *Polymer* **2005**, *46*, 877–886.
- (12) Prasse, T.; Cavaille, J. Y.; Bauhofer, W. Electric Anisotropy of Carbon Nanofibre/Epoxy Resin Composites due to Electric Field Induced Alignment. *Compos. Sci. Technol.* **2003**, *63*, 1835–1841.
- (13) Yun, S. H.; Yoo, S. M.; Sohn, B. H.; Jung, J. C.; Zin, W. C.; Kwak, S. Y.; Lee, T. S. Electrically Anisotropic Thin Films Consisting of Polymeric and Metallic Nanolayers from Self-Assembled Lamellae of Diblock Copolymers. *Langmuir* **2005**, *21*, 3625–3628.
- (14) Duxin, N.; Liu, F. T.; Vali, H.; Eisenberg, A. Cadmium Sulphide Quantum Dots in Morphologically Tunable Triblock Copolymer Aggregates. *J. Am. Chem. Soc.* **2005**, *127*, 10063–10069.
- (15) Wang, M. F.; Zhang, M.; Li, J.; Kumar, S.; Walker, G. C.; Scholes, G. D.; Winnik, M. A. Self-Assembly of Colloidal Quantum Dots on the Scaffold of Triblock Copolymer Micelles. *ACS Appl. Mater. Interfaces* **2010**, *2*, 3160–3169.
- (16) Zhang, M.; Wang, M. F.; He, S.; Qian, J. S.; Saffari, A.; Lee, A.; Kumar, S.; Hassan, Y.; Guenther, A.; Scholes, G.; Winnik, M. A. Sphere-to-Wormlike Network Transition of Block Copolymer Micelles Containing CdSe Quantum Dots in the Corona. *Macromolecules* **2010**, *43*, 5066–5074.
- (17) Nie, Z.; Fava, D.; Kumacheva, E.; Zou, S.; Walker, G. C.; Rubinstein, M. Self-Assembly of Metal-Polymer Analogues of Amphiphilic Triblock Copolymers. *Nat. Mater.* **2007**, *6*, 609–614.
- (18) Lu, H. B.; Liao, L.; Li, J. C.; Shuai, M.; Liu, Y. L. Hematite Nanochain Networks: Simple Synthesis, Magnetic Properties, and Surface Wettability. *Appl. Phys. Lett.* **2008**, *92*, 093102.
- (19) Na, Y. H.; Shibuya, T.; Ujiie, S.; Nagaya, T.; Orihara, H. Stripe Formation in an Immiscible Polymer Blend under Electric and Shear-Flow Fields. *Phys. Rev. E* **2008**, *77*, 041405.
- (20) Migler, K. B. String Formation in Sheared Polymer Blends: Coalescence, Breakup, and Finite Size Effects. *Phys. Rev. Lett.* **2001**, *86*, 1023–1026.
- (21) Pathak, J. A.; Davis, M. C.; Hudson, S. D.; Migler, K. B. Layered Droplet Microstructures in Sheared Emulsions: Finite-Size Effects. *J. Colloid Interface Sci.* **2002**, *255*, 391–402.
- (22) Pathak, J. A.; Migler, K. B. Droplet-String Deformation and Stability during Microconfined Shear Flow. *Langmuir* **2003**, *19*, 8667–8674.
- (23) Lin-Gibson, S.; Pathak, J. A.; Grulke, E. A.; Wang, H.; Hobbie, E. K. Elastic Flow Instability in Nanotube Suspensions. *Phys. Rev. Lett.* **2004**, *92*, 048302.
- (24) Malkin, A. Y.; Semakov, A. V.; Kulichikhin, V. G. Self-Organization in the Flow of Complex Fluids (Colloid and Polymer Systems) Part 1: Experimental Evidence. *Adv. Colloid Interface Sci.* **2010**, *157*, 75–90.
- (25) Zhu, Y. T.; Yang, X. D.; Yin, J. H.; Jiang, W. Droplet-Cluster Transition in Sheared Polyamide 6-Poly(styrene-ethylene-butadiene-styrene)-Polypropylene Ternary Blends. *Phys. Rev. E* **2010**, *82*, 031807.
- (26) Lee, C. G.; Wei, X. D.; Kysar, J. W.; Hone, J. Measurement of the Elastic Properties and Intrinsic Strength of Monolayer Graphene. *Science* **2008**, *321*, 385–388.
- (27) Balandin, A. A.; Ghosh, S.; Bao, W. Z.; Calizo, I.; Teweldebrhan, D.; Miao, F.; Lau, C. N. Superior Thermal Conductivity of Single-Layer Graphene. *Nano Lett.* **2008**, *8*, 902–907.
- (28) Geim, A. K. Graphene: Status and Prospects. *Science* **2009**, *324*, 1530–1534.
- (29) Stankovich, S.; Dikin, D. A.; Dommett, G. H. B.; Kohlhaas, K. M.; Zimney, E. J.; Stach, E. A.; Piner, R. D.; Nguyen, S. T.; Ruoff, R. S. Graphene-Based Composite Materials. *Nature* **2006**, *442*, 282–286.
- (30) Barroso-Bujans, F.; Boucher, V. M.; Pomposo, J. A.; Buruaga, L.; Alegria, A.; Colmenero, J. Easy-Dispersible Poly(glycidyl phenyl ether)-Functionalized Graphene Sheets Obtained by Reaction of “Living” Anionic Polymer Chains. *Chem. Commun.* **2012**, *48*, 2618–2620.
- (31) Huang, X.; Yin, Z. Y.; Wu, S. X.; Qi, X. Y.; He, Q. Y.; Zhang, Q. C.; Yan, Q. Y.; Boey, F.; Zhang, H. Graphene-Based Materials: Synthesis, Characterization, Properties, and Applications. *Small* **2011**, *7*, 1876–1902.
- (32) Liu, Z. F.; Liu, Q.; Huang, Y.; Ma, Y. F.; Yin, S. G.; Zhang, X. Y.; Sun, W.; Chen, Y. S. Organic Photovoltaic Devices Based on a Novel Acceptor Material: Graphene. *Adv. Mater.* **2008**, *20*, 3924–3930.
- (33) Bai, H.; Xu, Y. X.; Zhao, L.; Li, C.; Shi, G. Q. Non-Covalent Functionalization of Graphene Sheets by Sulfonated Polyaniline. *Chem. Commun.* **2009**, 1667–1669.
- (34) Eda, G.; Chhowalla, M. Graphene-based Composite Thin Films for Electronics. *Nano Lett.* **2009**, *9*, 814–818.
- (35) Montesi, A.; Pena, A. A.; Pasquali, M. Vorticity Alignment and Negative Normal Stresses in Sheared Attractive Emulsions. *Phys. Rev. Lett.* **2004**, *92*, 058303.
- (36) Mao, C.; Zhu, Y. T.; Jiang, W. Design of Electrical Conductive Composites: Tuning the Morphology to Improve the Electrical Properties of Graphene Filled Immiscible Polymer Blends. *ACS Appl. Mater. Interfaces* **2012**, *4*, 5281–5286.